THEORETICA CHIMICA ACTA

Theoret. Chim. Acta (Berl.) 51, 349–357 (1979)

The Molecular Electrostatic Potential of the B-DNA Helix

III. The Potential Due to the Sugar-Phosphate Backbone*

David Perahia, Alberte Pullman and Bernard Pullman

Institut de Biologie Physico-Chimique, Laboratoire de Biochimie Théorique associé au C.N.R.S., 13, rue P. et M. Curie, F-75005 Paris, France

The overlap multipole expansion procedure is utilized for the evaluation of the component of the electrostatic molecular potential of the B-DNA helix due to its sugar-phosphate backbone. The overall shape of the potential, its extension in space, the location of the minima and the differences in the values of the potential in particularly significant regions (minor and major grooves, vicinity of the phosphates) are indicated. The isopotential surfaces are practically cylindrical at distances larger than 15 Å from the helix axis but exhibit a more complex structure at shorter distances.

Key words: B-DNA backbone, electrostatic potential of ~

1. Introduction

In the previous papers of this series [1, 2] we have computed the electrostatic molecular potential around the guanine-cytosine and adenine-thymine base pairs *within* a B-DNA helix, using an appropriate mini-helix model. As a continuation of these studies we have now extended our computations to the evaluation of the potential in the inner and the outer regions of the double helix due to the sugar-phosphate backbone. The overall shape of the electrostatic potential, its extension in space, the location of the minima and the differences in the values of the potential in particularly significant regions (minor and major grooves, vicinity of the phosphates) have been investigated. These characteristics are expected, in particular, to provide indications on the possible binding sites for counterion distribution around DNA.

* This paper is dedicated to Professor H. Hartmann on the occasion of his 65th birthday.

0040-5744/79/0051/0349/$01.80

2. Procedure

The model considered in this study consists of a B-DNA double helix containing 11 repeating units constituted by sugar and phosphate components on both backbones. The geometry adopted is that given by Arnott *et al.* [3] for B-DNA. The model corresponds thus to a whole helical turn for each of the strands. The bases have not been included in the model so that this investigation aims essentially at the evaluation of the electrostatic potential created by the backbone of the nucleic acid. The contribution of the bases to the potential around DNA will be the subject of a subsequent article.

In the first stage all the electrostatic potentials are computed in a plane (P) perpendicular to the axis of the double helix and passing through the 6th phosphate belonging to one of the strands (Fig. 1). Such a plane leaves an equal number of units on each of its sides. In order to decrease the computational time, only four sugar units on each strand have been considered; they are the nearest ones to the plane P on both its sides. Such an approximation is justified by the fact that the long-range contributions of the sugars have negligible values when compared to the corresponding values of the negatively charged phosphate groups [4, 5].

A system of cylindrical coordinates centered on the axis of the helix has been adopted. The symbol r will be used for denoting the distance (in Å) from the axis in the plane P, and the symbol θ for the angle between a given direction and O–P6; positive values of θ correspond to an anticlockwise rotation in this plane (see Fig. 1).

The following complementary notations will be adopted: B' will denote the direction pointing toward the phosphorus atom in the plane under consideration ($\theta = 0°$). B ($\theta = 216°$) will denote the direction toward the projection on P of the closest phosphate to that plane on the complementary strand (see Fig. 2). M and m will denote the directions pointing toward the middle of the major and minor

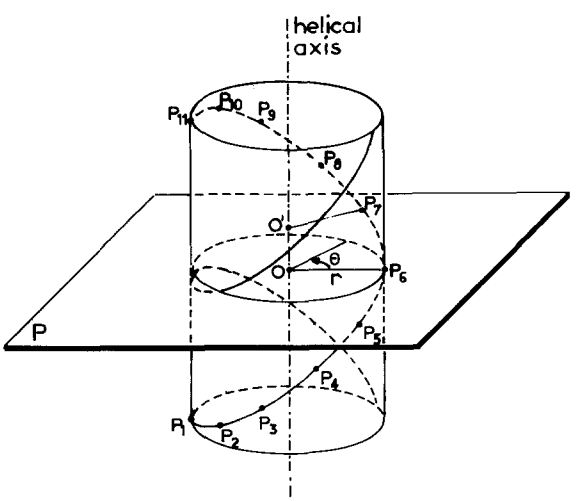

Fig. 1. Schematic view of the double helix, of the plane (P) of the computed potentials and notations considered in this study

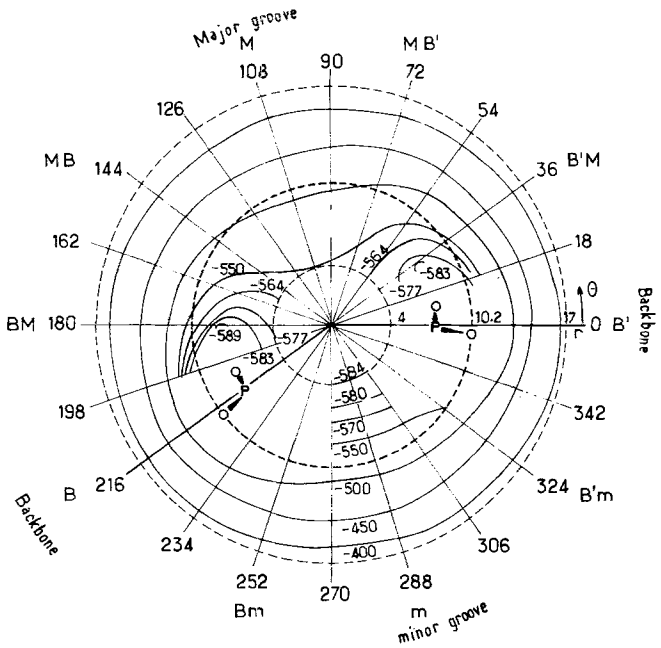

Fig. 2. Electrostatic isopotential curves (kcal/mole) in the plane *P*. Distances (*r*) from the axis of the helix (in Å) are indicated in the *B'* direction. The circle at $r = 10.2$ Å delimits the outer surface of the helix. The phosphorous *B'* is in the plane *P*. The orientation of the associated anionic oxygens is indicated

grooves; they correspond to $\theta = 108°$ and 288°, respectively. Intermediate directions will be denoted by an association of two letters: *BM* or *B'M* define the directions comprised between *B* or *B'*, and *M*, but closer to *B*; and *MB* or *MB'* the directions closer to *M*. *Bm* or *B'm* define, similarly, the directions comprised between *B* or *B'*, and *m*. All these directions are separated by rotations of 36° (see Fig. 2 for the illustration of these directions and the correspondence with the values of θ). Electrostatic potentials have also been computed in three other planes parallel to plane *P* and dividing *OO'* in equidistant segments (*OO'* corresponds to a unit height along the helical axis). They will be denoted as *P'*, *P''* and *P'''*, corresponding to increasing distances from *P*. These planes are separated from one another by a distance of 0.84 Å.

The computation of the molecular potentials has been performed by a superposition of all the potentials created by the constituents of the model considered (22 phosphates and 8 sugars). The overlap multipole expansion procedure (OMTP) has been used for the evaluation of the potentials [6–7]. The computations are thus limited to distances greater than 2 Å with respect to the constituent atoms which represent the limits of validity of the method [8]; in this way also no steric contacts may occur with a ligand atom included in the region delimited in this manner. The basis set used in the *ab initio* computation is the same as in the previous articles of this series [1–2].

3. Results and Discussion

3.1. Isopotentials in Planes Perpendicular to the Helical Axis

The electrostatic isopotentials obtained in plane P are presented in Fig. 2. The potentials have been computed in a region comprised between 4 Å and 16 Å from the helical axis, and in directions going from $\theta = 0°$ to 360°, with a step of 18°. The first striking feature of Fig. 2 is the large value obtained for the potentials in comparison to the potential obtained for a single phosphate unit, at 2 Å from its anionic oxygen in the B direction, which amounts to -111 kcal/mole). The increase is due to the large number of negatively charged phosphate groups considered in the model. The screening of the phosphate groups by cations and water will undoubtedly decrease these potentials appreciably [9, 10] and the study of this screening effect will be presented in a forthcoming paper. A second feature which may be noticed in our results is that the potentials are quite appreciable at the distances from the outer surface of the helix (where the anionic oxygens of the phosphate are located) considered in the figure. In fact the potentials computed for a few points farther apart from the surface (not indicated in Fig. 2) show the large extension of the potential in space: its value is still of the order of -180 kcal/mole at a distance of 30 Å, of 121 kcal/mole at a distance of 50 Å, of -91 kcal/mole at a distance of 70 Å, and falls down to -73 kcal/mole at a distance of 90 Å, to -46 kcal/mole at a distance of 150 Å and -20 kcal/mole at a distance of 350 Å.

A third feature to be mentioned concerns the shape of the isopotential curves obtained. Circles have been drawn (in dotted lines) on Fig. 2 at different distances (4, 10.2 and 17 Å from the helix axis) for the sake of comparison of the actual potential curves with circular ones. The circle at 10.2 Å indicates the outer limit of the DNA. The electrostatic isopotential curves at large distances (-400 and -450 kcal/mole) are almost circular. At shorter distances the shapes are elliptic (isopotential curve of -500 kcal/mole). The shape of isopotential curves situated at a distance close to 10.2 Å and below is more sensitive to the contributions of the nearest units. We have purposely interrupted those at the limit of regions where they were not computable because of the proximity of different types of atoms. It is observed that the -550 kcal/mole isopotential curve goes from the periphery of DNA (10.2 Å) toward its innermost region (4 Å), in a symmetric way with respect to the direction of the middle of the major groove ($\theta = 108°$). The potential minima (-583 and -589 kcal/mole) form very localized sites within this groove and originate from the contributions of the nearest anionic oxygens of the phosphates which are turned toward the same groove.

Regarding the region of the minor groove ($\theta = 288°$), the isopotential curves are short and parallel to each other. The fact that the sugar units are turned toward the minor groove limits the allowed region within this groove. The electrostatic potential value at 4 Å in the minor groove is very close to the minimum value obtained in the major groove at a larger distance.

The isopotential curves obtained in the planes P', P'' and P''' are similar to those of plane P, with only very slight differences which affect the values of the minima in

the major groove. In plane P' these minima become -600 and -593 kcal/mole; in the other planes they have intermediate values between -580 and -600 kcal/mole.

3.2. Potentials along the Directions Perpendicular to the Helical Axis

Because of the almost symmetric shapes obtained for the isopotential curves in Fig. 2 with respect to the *m–M* axis, we will only consider in this part of the study the directions *m*, *Bm*, *B*, *BM*, *MB* and *M*. The electrostatic potentials obtained along these directions are presented in Fig. 3. The global minimum is situated along the curve *BM* at a distance of almost 8 Å from the helical axis. At a distance smaller than 5.8 Å the potentials along the direction *m* become deeper than those on the curve *BM*. The least important directions are those pointing toward the region in the middle of the major groove (*M* and *MB*). For shorter distances ($r < 6$ Å) the potential curves may be subject to large perturbations due to the bases and those should then be added to the present ones. The study of the electrostatic potentials as a function of base composition will be presented in a forthcoming paper. We may already notice, however, that the atoms O2 of cytosine and thymine, N2 and N3 of guanine and N3 of adenine are located near the direction *m* at $r < 6$ Å, in a region which the present results indicate as being electrostatically favored for electrophilic attacks. On the contrary, the atoms N4 of cytosine, O4 of thymine, O6 of guanine and N6 of adenine are located near the *M* and *MB* directions which are electrostatically less favored by the backbone potential. N7 of adenine and guanine is located near the *BM* direction, which is slightly less favored than the *m* direction, at $r < 6$ Å.

At long distances from the helical axis the curves of Fig. 3 tend to approach each other, the largest difference between the potentials being of the order of 20 kcal/mole at $r = 16$ Å. This difference represents 5% of the total potential at this distance. At 12.2 Å from the helical axis this difference becomes appreciable, and is of the order of 90 kcal/mole. It decreases until 40 kcal/mole at $r = 4$ Å. Thus the largest difference between the potentials corresponds to the region close to the periphery of the double helix, and is clearly due to the strong local effects of the anionic oxygens.

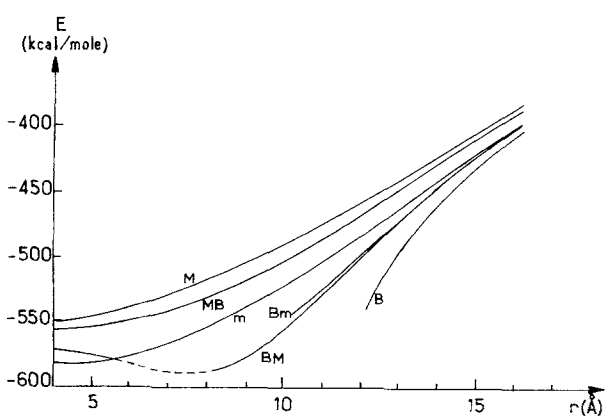

Fig. 3. Electrostatic potential curves in kcal/mole along selected directions perpendicular to the helical axis, in the plane *P*

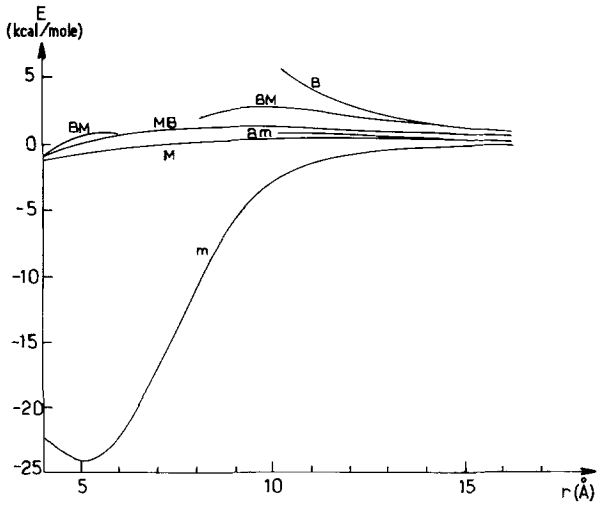

Fig. 4. Electrostatic potential (curves in kcal/mole) due to sugar components in the same directions as in Fig. 3

In order to put into evidence the contribution of the sugars we present in Fig. 4 the potentials produced by these components only. A large deepening of the potential is observed at $r = 5$ Å along the curve m, which contrasts with the other curves. This deepening is due to the contribution of the ring oxygens of the sugars which are all turned toward the minor groove.

3.3. Potentials around and along the Double Helix

The electrostatic potentials obtained on circles centered around the helical axis at different distances from it are presented in Fig. 5. It is observed that the most negative potentials along the curves are situated at their extremities when they are interrupted, or in front of the phosphates when they are continuous (B). The least negative potentials are situated in front of the middle of each groove (M and m). The most attractive regions for electrophiles are thus located in front of the phosphates or around them within the grooves. A large variation of the potentials is observed in the inner and border region of DNA ($r < 12.2$ Å). The variation becomes more and more flat in the outside region.

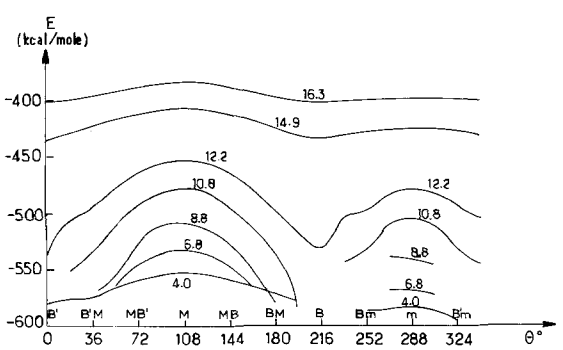

Fig. 5. Electrostatic potential curves in kcal/mole on circles, centered on the helical axis, in the plane P

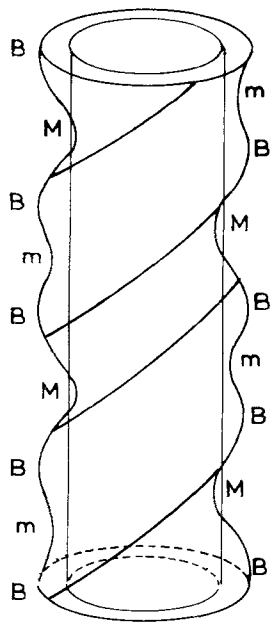

Fig. 6. Perspective view of an isopotential surface around B-DNA near its outer limit ($\simeq 10.2$ Å). The cylinder indicates this limit

The variations along directions parallel to the helical axis are identical to those of the curves of Fig. 5 for all the distances. The symbols in the abscissa are then representative of the positions considered along the double helix.

Extrapolating these data into a three-dimensional frame, it may be concluded that for distances larger than 15 Å from the helical axis, the electrostatic isopotentials form almost perfect cylinders, and that for shorter distances the cylinders show fluctuations of their surface potential which may reach 20%. A perspective view of the shape of the isopotential surface in the border region of the B-DNA is presented in Fig. 6 which encompasses four units of Fig. 1. This surface, which is essentially helicoidal (it evokes a wreathed column), presents major and minor grooves of different depths and widths. The global minima are encountered on going from the dark helicoidal lines on this surface toward the interior of the double helix.

4. Conclusions

The main conclusions which may be drawn from this study are the following: 1) The electrostatic potential around DNA is very strong and extends quite far from the helical axis; 2) The isopotential surfaces are practically cylindrical for distances larger than 15 Å from the helical axis, and are of helicoidal shape for shorter distances; 3) In the latter case major and minor grooves of potential are observed, corresponding to those of the B-DNA structure. The major groove of these surfaces is wider and deeper than the minor groove; 4) The global potential minima are located within the major groove near the phosphates at the proximity of the periphery of B-DNA and arise from the contribution of the anionic oxygens

of the phosphate groups which are turned toward the major groove; 5) Strong electrostatic potentials are observed in the inner region of the minor groove; a non-negligible contribution to their values is due to the ring oxygens of the sugar units, which, on both strands, are turned toward the minor groove.

Our results, which indicate at the same time the practical uniformity of the potential at a relatively small distance ($\simeq 6$ Å) from the outer limits of the DNA double helix and the existence of localized potential minima when we approach closer to that helix, are in accordance with the possibility of observing two types of interaction of metal cations with DNA: delocalized binding of an ionic cloud forming a positively charged atmosphere around the substrate and site-binding, localized, specific interaction. The exact aspect of the observed interaction will depend in each case on the nature of the ion and the solidity of its hydration shell [11–14]. Recent model computations from our laboratory [10, 15] indicate, in the case of the alkali and alkaline-earth cations, a competitivity between the "through-water" interaction of the fully hydrated cations and the "direct" interaction of the partially dehydrated cations with the phosphate anion, with, however, a certain advantage for the through-water binding. The present results suggest that the ("through-water") interaction of the hydrated cations in which the metal ion is situated in the zone of potential uniformity of DNA should be predominantly of the delocalized type. They do not exclude the possibility of localized direct binding of a partially dehydrated species. An example of the simultaneous occurrence of the two types of binding to DNA is offered by Mn^{2+} [11]. The specific binding corresponds to a chelation of the partially dehydrated cation (release of two water molecules) between the phosphate group and N7 of guanine. The location of this ion corresponds therefore to an intermediate position between the backbone and the middle of the major groove but closer to the backbone. Such a location corresponds to the position of the global potential minimum found in our study.

Another significance of our results can be found in relation to the attractive explanation given in methylation experiments for the recognition process between the *lac* repressor and operator DNA by Kolchinsky *et al.* [16]. Following these authors, the repressor initially binds into the minor groove of DNA in a non-specific interaction and proceeds to wander within this groove until it recognizes the operator. Such a sliding process appears very plausible in view of our isopotential surfaces in the vicinity of DNA which consist then of continuous helicoidal grooves.

References

1. Pullman, A., Zakrzewska, K., Perahia, D.: Intern. J. Quantum Chem. Quantum Biol. Symp., in press
2. Perahia, D., Pullman, A.: Theoret. Chim. Acta (Berl.) **50**, 351 (1979)
3. Arnott, S., Hukins, D. W. L.: Biochem. Biophys. Res. Commun. **47**, 1504 (1972)
4. Berthod, H., Pullman, A.: Theoret. Chim. Acta (Berl.) **47**, 59 (1978)
5. Berthod, H., Pullman, A.: Chem. Phys. Letters **32**, 233 (1975)
6. Dreyfus, M.: Thèse de 3è cycle, University of Paris (1970)
7. Pullman, A., Perahia, D.: Theoret. Chim. Acta (Berl.) **48**, 29 (1978)

8. Goldblum, A., Perahia, D., Pullman, A.: Intern. J. Quantum Chem. **15**, 121 (1979)
9. Pullman, A., Berthod, H.: Chem. Phys. Letters **41**, 205 (1976)
10. Berthod, H., Pullman, A.: Chem. Phys. Letters **46**, 249 (1977)
11. Manning, G. S.: J. Chem. Phys. **11**, 179 (1978)
12. Manning, G. S.: Quart. Rev. Biophys. **11**, 179 (1978)
13. Reuben, J., Shoporer, M., Gabbay, E. J.: Proc. Natl. Acad. Sci. USA **72**, 245 (1975)
14. Clement, R. M.: Biopolymers **12**, 405 (1973)
15. Pullman, A., Pullman, B., Berthod, H.: Theoret. Chim. Acta (Berl.) **47**, 175 (1978)
16. Kolchinsky, A. M., Mirzabekov, A. D., Gilbert, W., Li, L.: Nucl. Acids Res. **3**, 11 (1976)

Received January 22, 1979